# THERMOPHYSICAL PROPERTIES OF HYPOEUTECTIC, EUTECTIC AND HYPEREUTECTIC Al-Si AUTOMOTIVE ALLOYS UNDER AGEING TREATMENT

Ahmed Asif Razin[1], Dewan Sal-Sabil Ahammed[1],
Akib Abdullah Khan[1], Mohammad Salim Kaiser[2]

[1]*Department of Mechanical Engineering*
*Bangladesh University of Engineering and Technology*
*Dhaka-1000, Bangladesh*
[2]*Innovation Centre*
*International University of Business Agriculture and Technology*
*Dhaka-1230, Bangladesh*
*E-mail: dkaiser.res@iubat.edu*

*Received: 14 February 2023*
*Accepted: 19 December 2023*
*DOI: 10.59957/jctm.v59.i3.2024.22*

## ABSTRACT

*Influence of different levels of silicon under a variety of thermal treatment is investigated on the thermophysical behaviour of Al-Si-Cu-Mg automotive alloys. Conventional cast alloys are subjected to T6 heat treatment for age hardening. Hardness values, thermal conductivity along with microstructural observation under different heat-treated conditions are well thought-out to comprehend the ageing performance and the precipitation behaviour of the alloys. From these investigational results it is indicated that two successive hardening peaks take place in the aged alloys. Ageing sequence consists of different phases like a supersaturated solid solution, GP zones, intermediate β'', intermetallic β', equilibrium β and the Q phase but GP zones and the metastable phases are most likely responsible for these ageing peaks. Thermal conductivity decreases for these precipitates formation during ageing and increases for relieving the internal stress, dissolution of metastable phase and coarsening the precipitation of the alloys. Adding up of Si to the alloy showed earlier ageing peaks with higher intensities intended for its increasing properties of heterogeneous nucleation and diffusion kinetics. After ageing around at 200°C for four hours the alloys offer the height hardness. Microstructural study reveals that eutectic silicon makes the grain boundary coarsen and beyond the eutectic composition the star-shaped blocky primary Si is formed. Subsequent to ageing at 350°C for one hour the alloys reach completely recrystallized state.*

*Keywords: Al-Si alloys, T6 heat treatment, precipitates, age hardening, thermal conductivity, microstructure.*|

## INTROODUCTION

Al-Si cast alloys are lightweight materials having superior castability and exceptional mechanical properties. Owing to theses outstanding properties widely used in the automotive industries [1 - 3]. This type of alloys is classified based on the silicon content as hypoeutectic, eutectic and hypereutectic alloys where Si content less than 12 wt. %, 12 - 13 wt. % and higher than 13 wt. % respectively [4, 5]. Amount of Si plays significant role on the cast ability, hardness, wear as well as machinability of the alloys. Hypereutectic Al-Si alloys with higher Si addition have lower density, high-temperature resistance, wear resistance, corrosion resistance, specific stiffness and low thermal expansion. This is why there is great interest in the automobile industry to use this alloy instead of cast iron in engine parts [6, 7]. Some applications of Al-Si alloy include two main engine components, engine block and cylinder head along with high-performance automobile engine parts such as connecting rods, rocker arms, and valve retainers etc. Hypoeutectic Al-Si cast alloys used for small engine like motorcycle, eutectic alloys for medium engine like cars, microbus and hypereutectic alloys used

for the heavier engine like minibus [8]. Small amounts of Cu, Mg, Mn, Zn, and Ni are also alloyed to strengthen the Al-Si alloys. Additionally, Zr, Ti, Sc, Ce etc. as trace element are added for grain refinement of the alloys [9-12]. Sometimes the impurities such as Fe, Pb, Sn come from the melting surroundings like refractory furnaces linings, ladles, reactors etc. and these elements have an important influence on the properties of alloys [13].

When the Al-Si alloy contented minor alloying elements, Cu and Mg not only improve the mechanical properties but also make the alloy responsive to precipitation hardening. Therefore Al-Si-Cu-Mg alloys normally provide high age hardening response. To achieve advanced mechanical properties of this Al-Si automotive alloys Cu considered around 2 wt. % and Mg ranging from 0.3 to 1 wt % [14 - 16]. Thermal treatments of age-hardenable alloys include solutionizing, quenching and ageing, lead to changes in the nature and distribution of alloys ingredients. Properties of these alloys are dependent on both the time and temperature of ageing process. The outstanding thermal conductivity makes the alloy an appropriate alternative to cast iron for making engine components. Al-Si alloy also has the thermomechanical performance required for high engine operating temperatures and increased pressures [17, 18].

It is well recognized that the increased variation of silicon in these automotive alloys leads to a greater refinement towards eutectic silicon followed by primary silicon thereby changing the morphology of the matrix. The age hardening phenomenon depends on the size, distribution and coherence of the precipitated formed during ageing [19]. Not enough information is available of different Si effect on these alloys concerning the ageing behavior. Thus, the aim of this present study was to determine the influence of Si content on the ageing behaviour in terms of hardness, thermal conductivity as well as microstructural observation of Al-Si-Cu-Mg automotive alloys where Cu and Mg are kept constant. Hypoeutectic, eutectic and hypereutectic Al-Si automotive alloys were the major concern of this study but without and minor Si also considered for better concerning of these properties.

## EXPERIMENTAL

Commercial purity aluminium, copper, magnesium, and master alloy of Al-50 wt. % Si were taken to prepare the experimental hypoeutectic, eutectic and hypereutectic Al-Si automotive alloys. Without and minor Si another two alloys also considered for this experiment. Melting was done in a clay-graphite crucible using a natural gas-fired pit furnace. Degasser also used throughout the common melting process. The furnace temperature was always kept within 750 ± 10°C. Casting was done in a mild steel mould of size 20 mm x 200 mm x 300 mm and preheated at 250°C. Before pouring, the molten material was stirred for homogenization. The alloys composition was evaluated by means of a Shimadzu PDA 700 optical emission spectrometer, as follows in Table 1.

The cast alloys were homogenized at 450°C for 12 hours, solutionized at 535°C for 2 hours followed by salt water quenching at room temperature. First the alloys were machined to exfoliate the surface oxide layer and cut into 18 mm x 18 mm x 5 mm pieces. The samples were then subjected to isochronal and isothermal ageing for different routines and schedule respectively. For this an Electric Muffle Furnace JSMF-30T ranging 900 ± 3.0ºC was used. Following this, finished surface of the samples was prepared by polishing for hardness and conductivity measurements. Micro Vickers Hardness Tester, model: HV-1000DT was used to measure the samples microhardness where 1Kg load for 10 seconds

Table 1. Average chemical composition by wt. % from OES analysis of the experimental alloys.

| | Si | Cu | Mg | Fe | Ni | Pb | Zn | Mn | Ti | Al |
|---|---|---|---|---|---|---|---|---|---|---|
| Alloy 1 | 0.244 | 2.158 | 0.767 | 0.211 | 0.199 | 0.163 | 0.076 | 0.065 | 0.005 | Bal |
| Alloy 2 | 3.539 | 2.309 | 0.784 | 0.273 | 0.217 | 0.166 | 0.083 | 0.067 | 0.010 | Bal |
| Alloy 3 | 6.149 | 2.113 | 0.754 | 0.301 | 0.264 | 0.163 | 0.111 | 0.073 | 0.012 | Bal |
| Alloy 4 | 12.656 | 2.130 | 0.770 | 0.311 | 0.277 | 0.169 | 0.168 | 0.081 | 0.014 | Bal |
| Alloy 5 | 17.851 | 2.190 | 0.755 | 0.321 | 0.281 | 0.167 | 0.198 | 0.097 | 0.021 | Bal |

was applied for the knoop indenter. At least seven indentations were practiced from different locations on each polished sample. The electrical conductivity of the alloys was measured by an electrical conductivity meter, type 979, and the thermal conductivity was calculated from those data using the Wiedemann-Franz law [20]. As cast and various thermally treated samples were subjected to optical metallographic and SEM studies. Alloy samples were polished with alumina, etched with Keller's reagent and observed under a Versamet-II Microscope and a Jeol Scanning Electron Microscope type of JSM-5200 respectively.

## RESULTS AND DISCUSSION

### Age-hardening behavior

#### *Isochronal Ageing*

The experimental results of microhardness are plotted in Fig. 1, due to isochronal ageing of the Si varied solution treated Al-Si-Cu-Mg automotive alloys. Initially the alloys exhibit higher hardness with increased concentration of Si. This can be attributed to Si elements forming a supersaturated solid solution in the alloy matrix resulting in solid solution strengthening. Additionally, it refines grain structure as strength increases with decreasing grain size [21]. Double aging peaks with comparable profiles are observed for all when the alloys are subjected to aging treatments at different temperatures for one hour. Similar observations have also been reported by several investigators [14, 22, 23]. The precipitation behaviour of such alloys consists of the following sequence. These are formation of GP zones, homogeneous precipitation of intermediate phase θ″-$Al_2Cu$ and β″-$Mg_2Si$, heterogeneous precipitation of intermetallic phase θ′-$Al_2Cu$ and β′-$Mg_2Si$ and rod or plate-shaped equilibrium phase θ-$Al_2Cu$ and β-$Mg_2Si$. However, the GP zone and metastable phases are mainly responsible for strengthening the two aging peaks, respectively. The absolute alloy strength is attained just before precipitation of the incoherent θ and, β-platelets. It can also form Q-$Al_5Cu_2Mg_8Si_6$, π-$Al_9FeMg_3Si_5$ and β-$Al_5FeSi$ phases etc. which has a lower strength contribution than the θ and β phases. At the start of aging, fine and profuse GP zones distribute evenly in the matrix, and then their influence on strengthening is significant. Then again at the midway stage of aging metastable phases are created and kept semi-coherence with the matrix which resists the dislocation movement efficiently, thus having some strengthening effect [22]. At the transition stage from GP zones to metastable phases, these GP zones are significantly dissolved so the number of GP zones is significantly reduced. Whereas the metastable precipitates have not grown up and are too small to effectively resist the movement of dislocation. Consequently, the alloys have less age-hardening effect between the two aging peaks.

It can be observed that the intensity of aging response is higher for alloys with higher Si content and lowest for 0.2Si base alloy. It is clear that the Si linked precipitates are absent only form copper-rich phase θ-$Al_2Cu$ and S-$Al_2CuMg$ instead of the previously mentioned precipitates because it contains negligible amounts of Si. But the important fact is that the addition of Si not only extends the aging strength but also provides an earlier aging response. These situations can be classified because the presence of Si-phase in the matrix has a great influence on the diffusion of Cu. The nucleation and growth process of θ′ ($Al_2Cu$) phase occurs earlier since the precursors nucleate heterogeneously, contributing to a significant increase in aging kinetics and higher strength in the early aging stage. This may be related to the higher diffusion rate of Si and Mg elements compared to Cu atoms [24, 25]. In the final stage of aging, the effects of over-ageing lead to a sharp decrease in the hardness of the alloys associated with recovery, coarsening of particles inconsistent with the grains, as well as recrystallization.

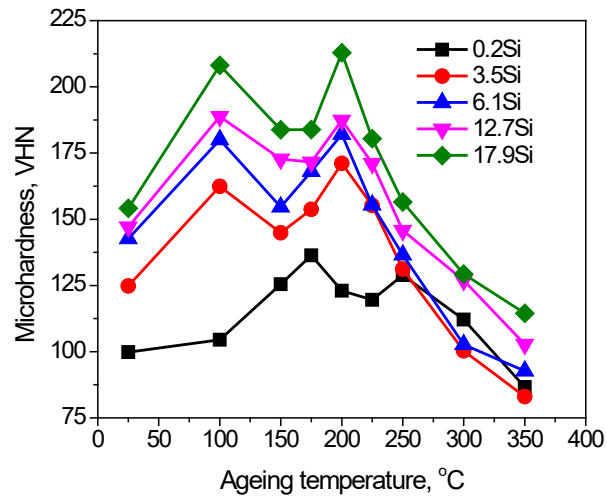


Fig. 1. Microhardness changes of the trial alloys under isochronal ageing treatment for one hour.

The derivative of thermal conductivity of the experimental alloys under the aforementioned identical conditions is displayed in Fig. 2. The conductivity curves of the alloys attain the similar in nature. At the initial stage of ageing treatment thermal conductivity slowly increases and sometimes decreases with ageing temperature. Strain recovery due to casting and GP zone dissolution results in increase in conductivity. However, fine precipitates of GP zone and metastable phase formation results in decrease in thermal conductivity of the alloys. The steep jump up of conductivity of the alloys beyond the ageing temperature at 200°C is considered to be due to dissolution of metastable phases and the precipitation coarsening which already formed in the matrix. Thermal conductivity of pure aluminium is around 210 W/m k. Addition of a variety of alloying elements like Si, Cu, Mg stay in solid solution distorts the lattice of the Al matrix and reduces the thermal transportation of electrons. On the other hand, Si-rich intermetallic increase with the Si contents and boost the scattering of electrons and phonons [13, 26].

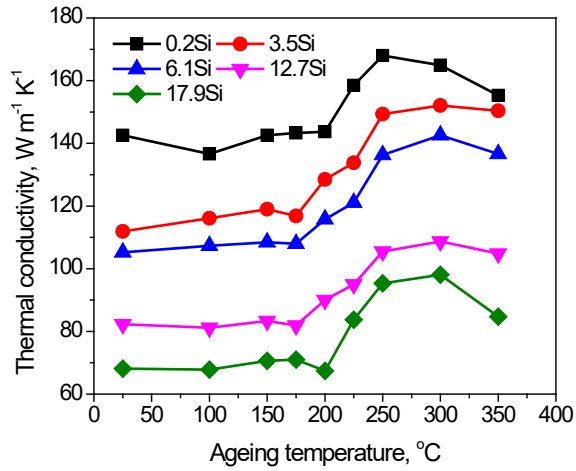


Fig. 2. Thermal conductivity changes of the trial alloys under isochronal ageing treatment for one hour.

### *Isothermal ageing*

Fig. 3 to Fig. 5 show the evolution of the hardness of the above alloys isothermally aged at 175, 200 and 225°C for different time respectively. In all cases with increasing ageing time, the hardness of the alloys first increases due to the formation of high-density GP zones that has strong strengthening capability, and then the hardness decreased due to dissolution of GP zone.

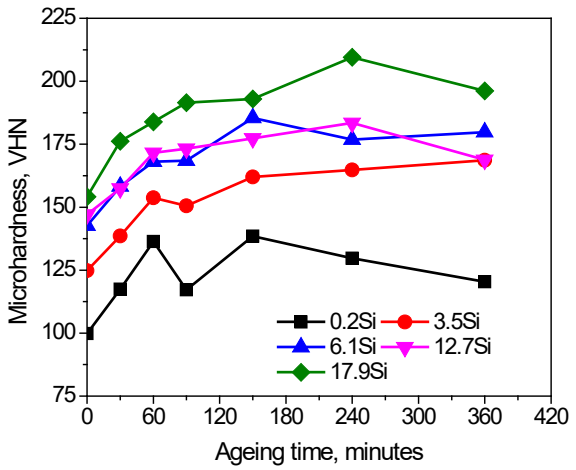


Fig. 3. Microhardness changes of the trial alloys under isothermal ageing treatment at 175°C.

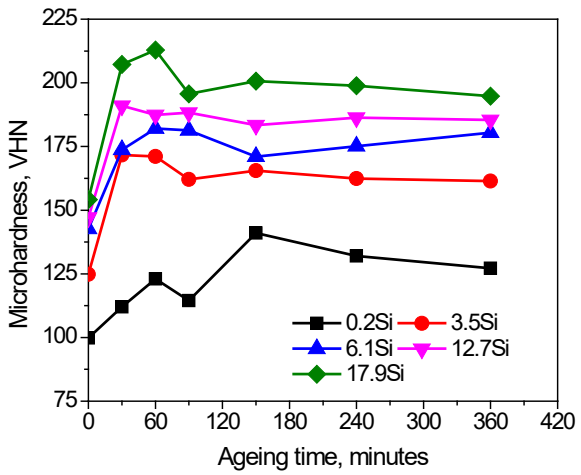


Fig. 4. Microhardness changes of the trial alloys under isothermal ageing treatment at 200°C.

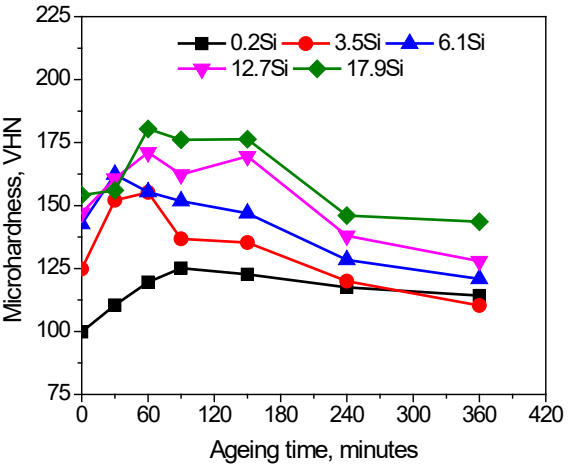


Fig. 5. Microhardness changes of the trial alloys under isothermal ageing treatment at 225°C.

As the GP zone dissolves, the precipitates grow to a stable phase, which has a relatively weak strengthening effect. Following this a subsequent strengthening effects are observed as associated with nanoscale metastable precipitates [27, 28]. At the higher ageing temperature for a long time the hardness decreases due to over ageing effects associated with grain and precipitation coarsening of the alloys. The ageing effect is more prominent at higher temperature for all the alloys. Comparing the relative effects of exposure time and temperature, exposure temperature has a relatively greater effect than exposure time. This indicates that the rate of diffusion is relatively faster by exposure temperature than by time. This result again supports the implication of the insignificant role of size the distribution of Si particles determines the nature and impact energy absorbed by the alloy precipitates [29]. From the combined effects of time and temperature it can be supposed that the optimum precipitation can be formed after ageing at 200°C for an exposure time 4h where maximum hardness can be achieved.

The average thermal conductivity values of the trail alloys aged isothermally at different temperatures are plotted in the following Fig. 6 to Fig. 8, where all graphs exhibit a general trend of increasing conductivity with aging time. However, at the initial stage of ageing around

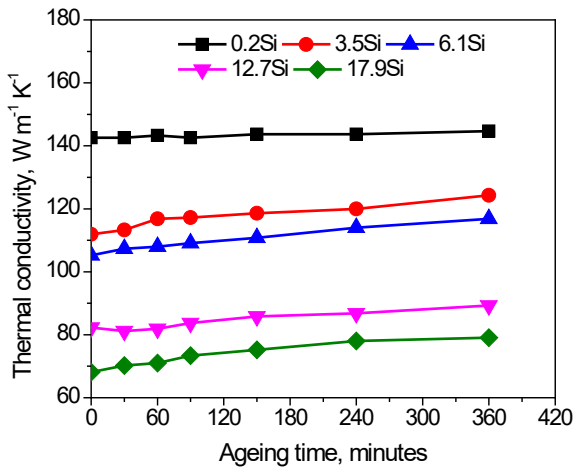


Fig. 6. Thermal conductivity changes of the trial alloys under isothermal ageing treatment at 175°C.

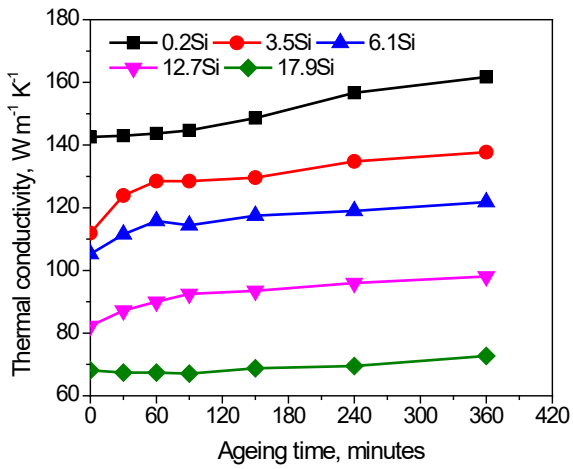


Fig. 7. Thermal conductivity changes of the trial alloys under isothermal ageing treatment at 200°C.

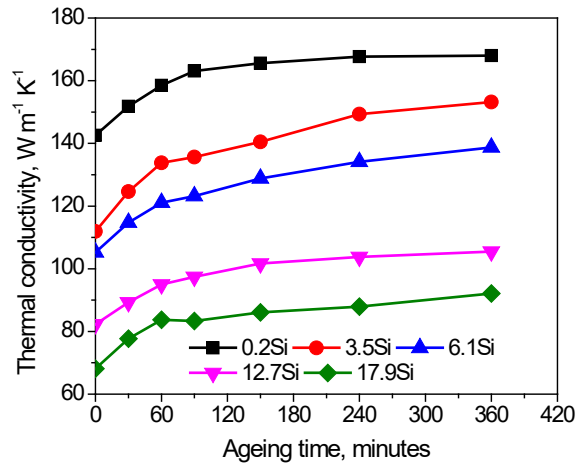


Fig. 8. Thermal conductivity changes of the trial alloys under isothermal ageing treatment at 225°C.

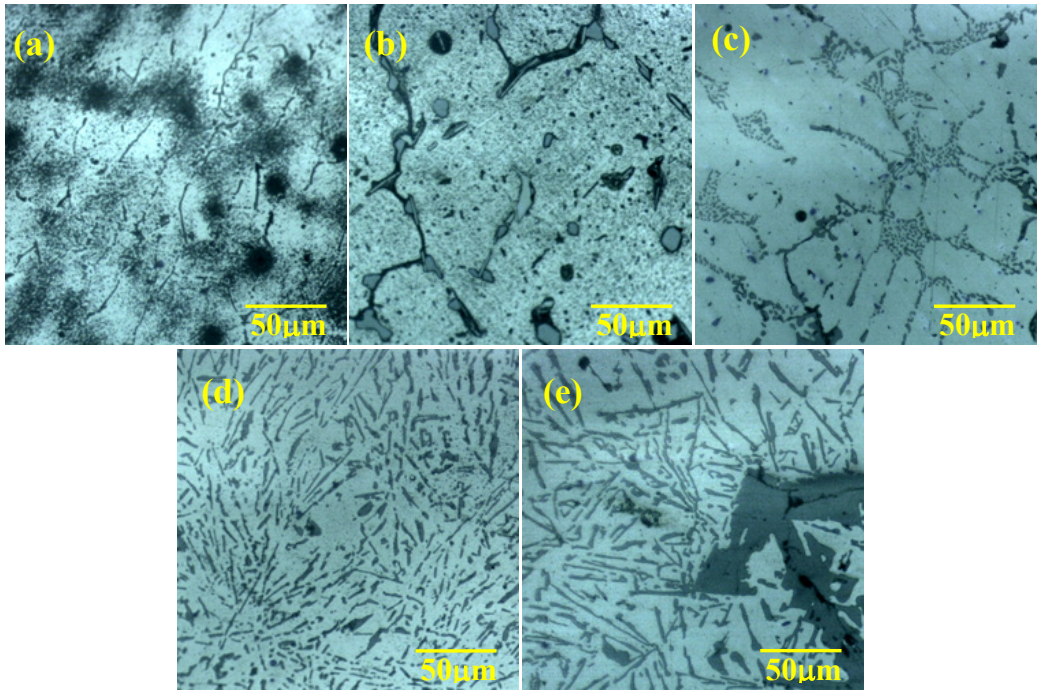


Fig. 9. Microstructure of solution treated (a) 0.2 Si, (b) 3.5 Si, (c) 6.1 Si, (d) 12.7 Si, and (e) 17.9 Si automotive alloy.

at two hours some fluctuating nature in conductivity of the alloys is noted. There are two things are related with this up down values of conductivity. It is already point out that GP zone and different precipitation formation reduces the conductivity of the alloys and stress reliving and recovery increase the conductivity of the alloys. So, the summation of these results is displayed in the graph. At higher ageing time the increases of the conductivity fully relater with precipitation and grain coarsening of the alloys. Fine precipitates make the alloys defect which hinder the electron movement and coarsen precipitates losses the efficiency hence the lower and higher conductivity. As the aging temperature increases, the diffusion processes are more accelerated and the effect of temperature is more prominent than that of time. So the rate of increasing the conductivity is higher and happened earlier at higher ageing temperature [25, 30].

**Optical Microscopy**

The effect of Si on the microstructure is demonstrated in Fig. 9, while the experimental automotive alloys are solutionized at 535°C for 2h. The microstructures of the 0.2 Si base alloy consists of mainly primary Al dendrite with a few numbers of different elements like Cu, Mg stay in solid solution (Fig. 9(a)). These are uniformly distributed into Al-matrix because of the solidification under rapid cooling [31, 32]. With addition of Si the eutectic phases start on in the microstructure of the alloys and make the grain boundary coarsen (Fig. 9(b) and 9(c)). The variation of silicon led to more degree of refinement and at the eutectic compassion appears with an elongated needle-like structure of Si (Fig. 9(d)) [33]. Beyond the eutectic composition 17.9Si added automotive alloy star-shaped blocky primary silicon is formed in the cast alloys (Fig. 9(e)). It is conspicuous from the microstructures that there is low density of needle-like Si near the primary Si phase, which dictates a solute lean area in silicon near the primary Si and matrix interface [34]. It has already been stated that the alloys without different amounts of Si consist of dissolved micro-segregation Cu, Mg and impurity elements that form a supersaturated solid solution in the alloy matrix which take part to produce a large number of reinforced precipitates during the subsequent aging process. But these fine precipitates cannot able exposed via this type of photography [35].

The effects of ageing temperature for one hour at 350°C on grain structure of the above-mentioned alloys are revealed in the Fig. 10. In most cases, equiaxed

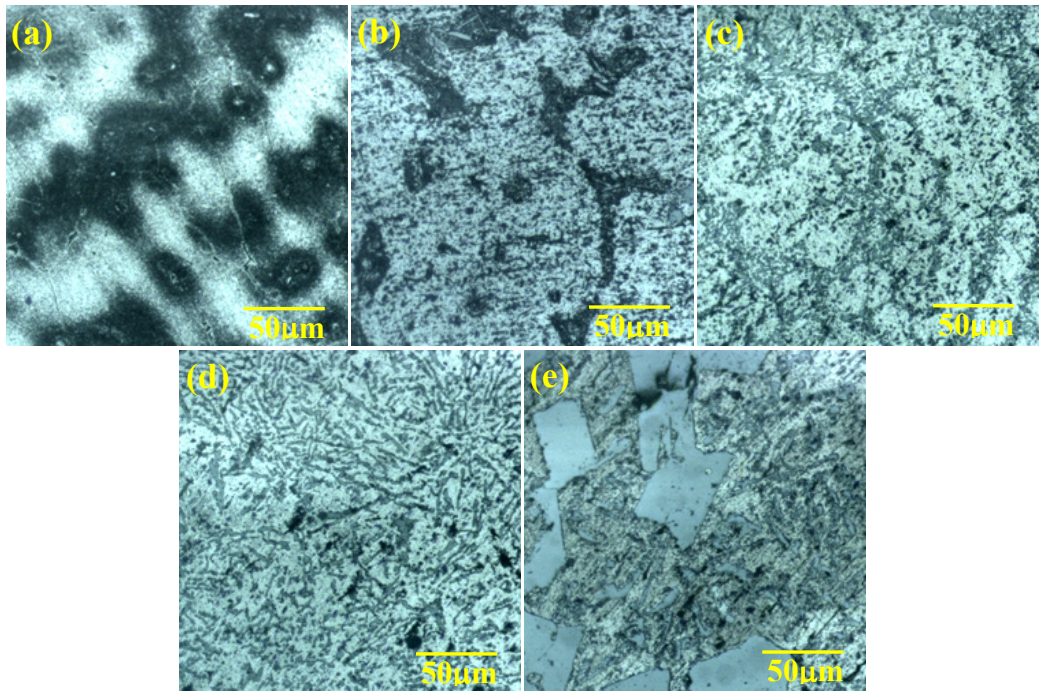


Fig. 10. Microstructure of solution treated followed by ageing at 350°C for one hour (a) 0.2 Si, (b) 3.5 Si, (c) 6.1 Si, (d) 12.7 Si, and (e) 17.9 automotive alloy.

grains are observed where the backgrounds of the microstructure are not too clear as the microstructure of the prior solution treated alloys are displayed. At this temperature applied for one hour, the dendrites give the impression of dissolution in addition to intermetallic coarsening occurred which homogeneously distributed into the matrix [36]. Consequently, the microstructures of all the alloys turn to equiaxed grains. In case of base alloy, the α-Al increases due to intermetallic aggregation and is uniformly distributed along the matrix (Fig. 10(a)). Addition of Si like 3.5 and 6.1 wt. %, eutectic Si phases are clearly seen in to the uniformly distributed aggregated intermetallic as it is not dissolved at this ageing condition (Fig. 10(b) and 10(c)). In the alloy with the addition of Si, fine distributions of particles separated from the Al matrix and Si particle segregation along the grain boundaries are seen. Then again, eutectic niddle-like Si in the defused aluminium matrix are observed in the microstructure of 12.7 Si alloy (Fig. 10(d)). Due to the existence of Cu, Mg and other impurities, at this ageing condition a huge number of complex intermetallic phases occurred together with the eutectic. Both blocky primary and eutectic plate-like Si phases mounted in the aluminium matrix are observed in the optical micrograph of the 17.9 Si added alloy (Fig. 10(e)).

**Scanning Electron Microscopy:**

Fig. 11 shows typical SEM micrographs of as-cast alloys subjected to T6 heat treatment so as to consist of a solutionizing at 535°C for 2h followed by rapid cooling and then an aging at 200°C for four hours. The microstructures of the 0.2 Si alloy exists the α-Al phase with different intermetallic particles distribute with in a granular and grain boundary (Fig. 11(a)) [37]. As the Si increases, eutectic phases begin to appear in the alloys as shown in Fig. 11(b) to (d). Due to the incessant of silicon content, the metallographic structure is evidence for more and additional eutectic silicon. A number of eutectic silicon grains are clearly uneven and elongated, and the α-Al matrix phase is alienated by the eutectic silicon phase, which is dispersed in chunks. They are needle-like and platelet eutectic Si distributing at the grain boundary which makes the grain boundary coarsens [16, 37]. At the eutectic composition, microstructural depiction reveals the main constituent of α-Al dendrites along with the elongated needle-like structure of silicon. Beyond the eutectic composition, the 17.9 Si added automotive alloy shows the star-shaped blocky primary Si on the background of an elongated needle-like eutectic structure (Fig.11(e)). The quantity of eutectic needle Si close to the primary Si is low because

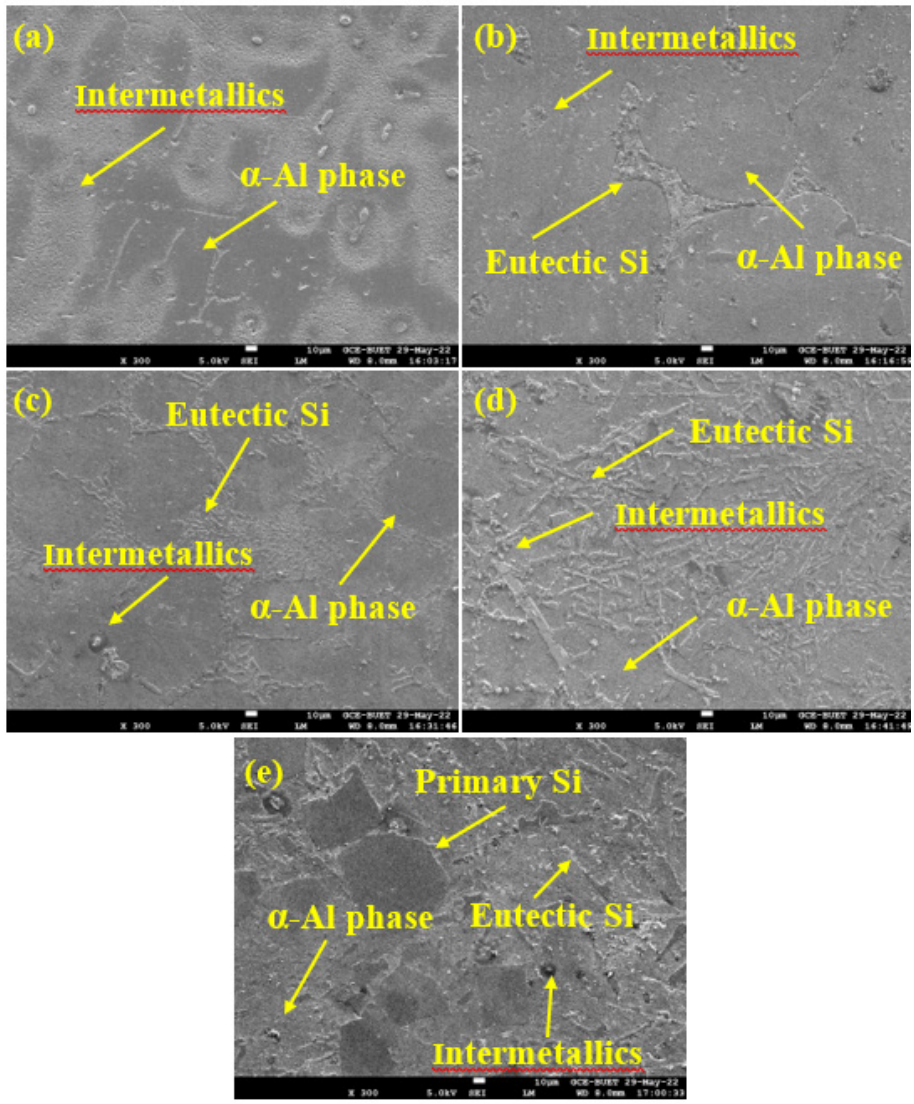


Fig. 11. SEM images of different Si added automotive alloys aged at 200°C for four hours (a) 0.2 Si, (b) 3.5 Si, (c) 6.1 Si, (d) 12.7 Si and (e) 17.9 Si.

it captures some fraction of Si indicating a solute lean region near the primary Si phase as also shown in the optical microstructure [38 - 40].

## CONCLUSIONS

Different levels of silicon together with heat treatment are investigated on the hardness, thermal conductivity and the microstructural change of Al-based automotive alloys. The study points out that:

- Two consecutive hardening peaks are generated in the aged alloys. Ageing sequence consists of different phases but GP zones and the metastable phases are associated for these ageing peaks. The main strengthening phases are θ-$Al_2Cu$, β-$Mg_2Si$ and Q-$Al_5Cu_2Mg_8Si_6$. The Si rich intermetallic make the difference of strengthening properties when Si is alloyed to this alloy. Adding up of Si showed earlier ageing peaks with higher intensities by its increasing properties of heterogeneous nucleation and diffusion kinetics. The optimum hardness of the alloys can be achieved after aging around at 200°C for four hours.
- Thermal conductivity of the alloys decreases with the Si concentration as form the higher Si-rich intermetallic along with others that reduce the heat transportation behaviour of electrons and phonons.

But it decreases during ageing for this precipitation formation and increases for relieving the cast internal stress, metastable phase dissolution and coarsening the precipitates in to the alloys.

- The addition of silicon into these types of automotive alloys led to more degree of eutectic silicon and makes the grain boundary coarsen. When the silicon content increased further than the eutectic composition, the primary silicon similar to star-shaped blocky is formed in the cast. Subsequent to ageing at 350°C for one hour create fully re-crystallized grains.

***Acknowledgement***

*This study is supported by the ME department of Bangladesh University of Engineering and Technology, Dhaka-1000. Thanks to DAERS office providing the workshop facilities.*

**REFERENCES**

1. I. J. Polmear, Light Alloys-Metallurgy of the Light Metals, 3rd edition, Arnold, UK, 1995.
2. P. Zhou, D. Wang, H. Nagaumi, R. Wang, X. Zhang, X. Li, H. Zhang, B. Zhang, Microstructural Evolution and Mechanical Properties of Al-Si-Mg-Cu Cast Alloys with Different Cu Contents, Metals, 13, *1*, 2023, 1-13.
3. M.S. Kaiser, Corrosion behavior of Al-12Si-1Mg automotive alloy in acidic, alkaline and salt media containing Zr traces, J. Chem. Technol. Metall., 54, 2, 2019, 423-430.
4. J.R. Davis, Light Metals and Alloys, Alloying: Understanding the Basics, 1st edition, ASM International, Ohio, USA, 2001.
5. M.A. Nur, A.A. Khan, S.D. Sharma, M.S. Kaiser, Electrochemical Corrosion Performance of Si Doped Al-Based Automotive Alloy in 0.1 M NaCl Solution, Journal of Electrochemical Science and Engineering, 12, 3, 2022, 565-576.
6. G. Mathers, The Welding of Aluminium and its Alloys, 1st edition, Woodhead Publishing, Sawston, Cambridge, UK, 2002.
7. M.S. Kaiser, Effects of solution treatment on wear behaviour of Al-12Si-1Mg piston alloy containing trace Zr MAYFEB, J. Mater. Sci., 1, 2016, 27-38.
8. M. Javidani, D. Larouche, Application of cast Al-Si alloys in internal combustion engine components, International Materials Reviews, 59, 3, 2014, 132-158.
9. M.N.E. Efzan, H.J. Kong, C.K. Kok, Review: Effect of Alloying Element on Al-Si Alloys, Advanced Materials Research, 845, 2013, 355-359.
10. M.S. Kaiser, A.S.W. Kurny, Effect of scandium on the grain refining and ageing behaviour of cast Al-Si-Mg alloy, Iranian Journal of Materials Sciences and Engineering, 8, 4, 2011, 1-8.
11. H.S. Abdo, A.H. Seikh, J.A. Mohammed, M.S. Soliman, Alloying Elements Effects on Electrical Conductivity and Mechanical Properties of Newly Fabricated Al Based Alloys Produced by Conventional Casting Process, Materials, 14, 14, 2021, 1-10.
12. S.I. Park, S.Z. Han, S.K. Choi, H.M. Lee, Phase Equilibria of $Al_3$(Ti, V, Zr) Intermetallic System, Scripta materialia, 34, 11, 1996, 1697-1704.
13. M.S. Kaiser, Effect of trace impurities on the thermoelectric properties of commercially pure aluminum, Materials Physics and Mechanics, 47, 4, 2021, 582-591.
14. S. Toschi, Optimization of A354 Al-Si-Cu-Mg Alloy Heat Treatment: Effect on Microstructure, Hardness, and Tensile Properties of Peak Aged and Overaged Alloy, Metals, 8, 11, 2018, 1-16.
15. H. Mao, X. Bai, F. Song, Y. Song, Z. Jia, H. Xu, Y. Wang, Effect of Cd on Mechanical Properties of Al-Si-Cu-Mg Alloys under Different Multi-Stage Solution Heat Treatment, Materials (Basel), 15, 15, 2022, 1-14.
16. M.S. Kaiser, Effect of solution treatment on the age hardening behaviour of Al-12Si-1Mg-1Cu piston alloy with trace Zr addition, Journal of Casting and Materials Engineering, 2, 2, 2018, 30-37.
17. S.S. Ahn, S. Pathan, J.M. Koo, C.H. Baeg, C.U. Jeong, H.T. Son, Y.H. Kim, K.H. Lee, S.J. Hong, Enhancement of the Mechanical Properties in Al-Si-Cu-Fe-Mg Alloys with Various Processing Parameters, Materials, 11, 11, 2018, 1-12.
18. M.S. Kaiser, Solution Treatment Effect on Tensile, Impact and Fracture Behaviour of Trace Zr Added Al-12Si-1Mg-1Cu Piston Alloy, Journal of the Institution of Engineers, India, Series D, 99, 1, 2018, 109-114.
19. S.P. Nikanorov, M.P. Volkov, V.N. Gurin, Y.A. Burenkov, L.I. Derkachenko, B.K. Kardashev,

L.L. Regel, R. Wilcox, Structural and mechanical properties of Al–Si alloys obtained by fast cooling of a levitated melt, Mater. Sci. Eng. A, 390, 1-2, 2005, 63-69.
20. G.V. Chester, A. Thellung, The Law of Wiedemann and Franz, Proceedings of the Physical Society, 77, 5, 1961, 1005-1013.
21. D.G. Eskin, Decomposition of supersaturated solid solutions in Al-Cu-Mg-Si alloys, J. Mater. Sci. 38, 2, 2003, 279-290.
22. H. Mao, X. Bai, F. Song, Y. Song, Z. Jia, H. Xu, Y. Wang, Effect of Cd on Mechanical Properties of Al-Si-Cu-Mg Alloys under Different Multi-Stage Solution Heat Treatment, Materials, 15, 2022, 1-14.
23. M. Zamani, S. Toschi, A. Morri, L. Ceschini, S. Seifeddine, Optimisation of heat treatment of Al-Cu-(Mg-Ag) cast alloys, J. Therm. Anal. Calorim. 139, 12, 2020, 3427-3440.
24. N.Q. Vo, D.C. Dunand, D.N. Seidman, Role of silicon in the precipitation kinetics of dilute Al-Sc-Er-Zr alloys, Mater. Sci. Eng. A, 677, 2016, 485-495.
25. A.M.A. Mohamed and F.H. Samuel, A Review on the Heat Treatment of Al-Si-Cu/Mg Casting Alloys, IntechOpen, London, UK, 2012.
26. M.S. Kaiser, Role of excessive iron on hyper-eutectic Al-Si automotive alloy: A Review, J. Mater. Eng. Struct., 8, 2, 2021, 241-251.
27. E. Sjolander, S. Seifeddine, The heat treatment of Al–Si-Cu-Mg casting alloys, J. Mater. Process. Technol., 210, 10, 2010, 1249-1259.
28. M.S. Kaiser, S.H. Sabbir, M. Rahman, M.S. Kabir, M.A. Nur, Heat treatment effect on the physical and mechanical properties of Fe, Ni and Cr added hyper-eutectic Al-Si automotive alloy, J. Chem. Technol. Metall., 55, 2, 2020, 409-416.
29. R.N. Kumar, T.R. Prabhub, C Siddaraju, Effect of thermal exposure on mechanical properties hypo eutectic aerospace grade aluminium-silicon alloy, IOP Conf. Series: Materials Science and Engineering, 149, 2016, 1-8.
30. J.K. Chen, H.Y. Hung, C.F. Wang, N.K. Tang, Effects of casting and heat treatment processes on the thermal conductivity of an Al-Si-Cu-Fe-Zn alloy, Int. J. Heat Mass Transf., 105, 2017, 189-195.
31. K. Liu, X. Cao, X.G. Chen, Effect of Mn, Si, and Cooling Rate on the Formation of Iron-Rich Intermetallics in 206 Al-Cu Cast Alloys, Metall. Mater. Trans. B, 43, 5, 2012, 1231-1240.
32. T.T. Alshammari, H.F. Alharbi, M.S. Soliman, M.F. Ijaz, Effects of Mg Content on the Microstructural and Mechanical Properties of Al-4Cu-xMg-0.3Ag Alloys, Crystals, 10, 895, 2020, 1-13.
33. S.P. Nikanorov, M.P. Volkov, V.N. Gurin, Y.A. Burenkov, L.I. Derkachenko, B.K. Kardashev, L.L. Regel, W.R. Wilcox, Structural and mechanical properties of Al–Si alloys obtained by fast cooling of a levitated melt, Mater. Sci. Eng. A, 390, 1-2, 2005, 63-69.
34. M.R. Alawandi, S.S. Khaji, D.M. Goudar, Microstructure and Mechanical Properties of Spray Formed and Hot-Pressed Hypereutectic AlSi Alloy, Research & Development in Material Science, 11, 1, 2019, 1134-1140.
35. G.G. Sirata, K. Wacławiak, M. Dyzia, Mechanical and Microstructural Characterization of Aluminium Alloy, EN AC-Al Si12CuNiMg, Arch. Foundry Eng., 22, 3, 2022, 34-40.
36. M. Liu, T. Wada, A. Suzuki, N. Takata, M. Kobashi,M. Kato, Effect of Annealing on Anisotropic Tensile Properties of Al-12 % Si Alloy Fabricated by Laser Powder Bed Fusion, Crystals, 10, 11, 2020, 1-14.
37. L. Li, Y. Zheng, Y. Chen, J. Feng, C. Li, L. Chen, L. Zuo, Y. Zhang, Study on Microstructure Distribution of Al-Cu-Mg Alloy in Squeeze Casting Process, J. Phys. Conf. Ser., 2338, 2022, 1-6.
38. S. Channappagoudar, K. Aithal, S. Narendranath, V. Desai, M. Pudukottah,, Effect of combined grain refinement and modification on microstructure and mechanical properties of hypoeutectic, eutectic and hypereutectic Al-Si alloys, J. Microstruct. Mater. Prop., 10, 3/4, 2015, 274-284.
39. M.S. Kaiser, S. Dutta, Comparison of corrosion behaviour of commercial aluminium engine block and piston in 3.5 % NaCl solution, Advances in Materials Science and Engineering: An Intern. J.,1, 1, 2014, 9-17.
40. V. Dyakova, Y. Kostova, V. Manolov, P. Kuzmanov, I. Panov, A. Velikov, B. Dochev, Comparative study of the influence of some nanomodifiers on the microstructure and corrosion properties of AlSi18 alloy, J. Chem. Technol. Metall., 56, 1, 2021, 205-213.